Fading Characterization of 73 GHz Millimeter-Wave V2V Channel Based on Real Measurements

Hui Wang[1], Xuefeng Yin[1,2(✉)], Xuesong Cai[1], Haowen Wang[3], Ziming Yu[4], and Juyul Lee[5]

[1] College of Electronics and Information Engineering, Tongji University, Shanghai, China
{l252759,yinxuefeng,caixuesong}@tongji.edu.cn
[2] National Computer and Information Technology Practical Education Demonstration Center, Tongji University, Shanghai, China
[3] Shanghai Research Center for Wireless Communications (WiCo), Shanghai, China
haowen.wang@wico.sh
[4] 5G Research Department, Huawei Technologies Corporation, Chengdu, China
yuziming@huawei.com
[5] Electronics and Telecommunications Research Institute (ETRI), Daejeon, South Korea
juyul@etri.re.kr

Abstract. In this work, a recently conducted measurement campaign for millimeter wave (mm-wave) vehicle to vehicle (V2V) propagation channel characterization is introduced. Two vehicles carrying a transmitter (Tx) and a receiver (Rx) respectively were driven towards each other at an average speed of 60 km/h in an urban area of Jiading District, Shanghai, China. The measurement was conducted with 409.6 MHz bandwidth at center frequency 73 GHz. The parameters investigated include the large-scale fading and small-scale fading coefficients. Specifically, a 2-slope path-loss model was proposed. Six kinds of distributions of analytical expressions were used to fit the fast fading distribution. The results show that the fast fading distribution changes from Rician to Nakagami, finally to lognormal with the distance between the Tx and the Rx increases.

Keywords: Vehicle to vehicle communication · Channel measurement Millimeter-wave · Channel fading characterization

1 Introduction

Mm-wave communications are going to be used for V2V communications [1]. Recently, the mm-wave V2V communications have been paid a tremendous attention. This is due to the fact that the mm-wave communication is expected to enable gigabyte per second data transmission for the future intelligent transportation systems. In such systems, a large amount of sensors are going to be deployed in the vehicles.

Furthermore, in order to realize unmanned manoeuvered vehicle technologies, big data needs to be exchanged between terminals and the cloud. For these applications, it is important to develop V2V mm-wave communication systems and techniques. As a fundamental research, the channel characterization for the mm-wave frequency bands is important for understanding the wave propagation in a variety of vehicular scenarios.

The reasons to investigate the propagation channel characteristics for mm-wave channels are as follows: Assuming that mm-wave propagation occurs along straight rays, this ray-alike propagation and the high attenuation of the mm-wave may jointly lead to the effect that the propagation does not involve multiple bounces. For the outdoor V2V scenario, it can be expected that there are not many multipath components existing in the channel, mainly resulting from the high attenuation and the directionality of antennas [2–4]. Meanwhile, the rapidly varying environment can introduce non-stationarity into the channel. Therefore, how to maintain a stable connection between the Tx and the Rx that are installed in different vehicles is of great importance for the design and performance evaluation of V2V communication systems.

V2V communications have been a hot-spot for research and industry as the rapid development of unmanned technologies. Channel models established so far can be divided into two classes: the simulation-based models and the measurement-based models. In the former category, the so-called geometrical scattering models are widely investigated. Most of them based on the assumption that scatterers are distributed either regularly, e.g. on one-ring, two-rings, elliptical ring, cylinder, ellipsoid, and etc., or irregularly [5, 6]. With the ideal assumptions of scatterer distributions, channel characteristics are derived which constitute a series of geometry-based stochastic models [7–15]. In the measurement based category, most V2V measurements are conducted at sub-6 GHz band [16–21]. Only few researchers conducted the mm-wave V2V channel measurements. For instance, the impact of interference from side lanes was studied in [22]. The time varying K-factor under the influence of velocity, vibrations and road quality was illustrated in [23]. The blockage characteristics including delay, angular spread and blockage loss was investigated in [24]. These studies facilitate evaluating system performance analytically and alleviate the difficulties in designing communication techniques. However, as far as we concerned, the fading characterization of V2V channel at 73 GHz has not been experimentally investigated based on measurements due to the expensive cost of equipments and the difficulties of conducting measurements.

In our work, a road measurement of V2V channel at center frequency of 73 GHz was carried out. The large-scale channel parameters such as path loss and the small-scale channel parameters e.g. fast fading coefficients are investigated. Furthermore, a 2-slope path loss model was proposed in the work and the statistical characteristics of shadowing and fast fading are investigated. Six types of distribution functions are used to find the best-fit for fast fading coefficients. Rician K-factor and m-parameter of Nakagami are calculated for modelling and in-depth analysis.

The rest of the work is organized as follows: In Sect. 2, we introduce the measurement equipments and scenarios. In Sect. 3, the measurement results are analysed. Finally, the conclusive remarks are presented in Sect. 4.

2   Measurement Equipment and Scenarios

In the measurement campaign, the WiCo mm-wave channel sounder was adopted. A PN sequence modulated with QPSK and raised-cosine pulse-shaped was exploited to sound the channel at the center frequency of 73 GHz. The sequence length was 4095 chips. The bandwidth was 409.6 MHz. Two rubidium clocks were used to synchronize the Tx and the Rx. GPS devices were used to record position information which can be used for location mapping. Two identical antennas with 10° Half-Power-Bandwidth (HPBW) and gains of 25 dBi were adopted as Tx and Rx. The front view of sounder, the side view of horn antenna are shown in Fig. 1. As illustrated in Fig. 2, two sets of devices were placed into two 7-passenger cars separately. In order to obtain better signal-to-noise ratio (SNR), the Tx and Rx antennas were mounted on the car roof, which aims to avoid the car penetration loss. The heights of both antennas were around 1.5 m. Figure 3 shows the satellite map of the measurement area. The yellow line denotes the route of measurement. Two cars accelerated from 0 to 60 km/h and then were driven toward each other at a stable speed. The measurement campaign was

(a) The front view of WiCo sounder   (b) The side view of horn antenna used in measurement campaign

Fig. 1.   Pictures of measurement devices

(a)   (b)

Fig. 2.   Photographs taken when the equipments are placed in car.

conducted in the urban area of Jiading district, Shanghai. The route is adjacent to an underground station and business buildings. Hence, the traffic was busy during the measurements. The whole route is about 1.05 km. The route contains four lanes among where no obstacles lie. The maximum speed of the car is 60 km/h. Some of the measurement specifications are listed in Table 1.
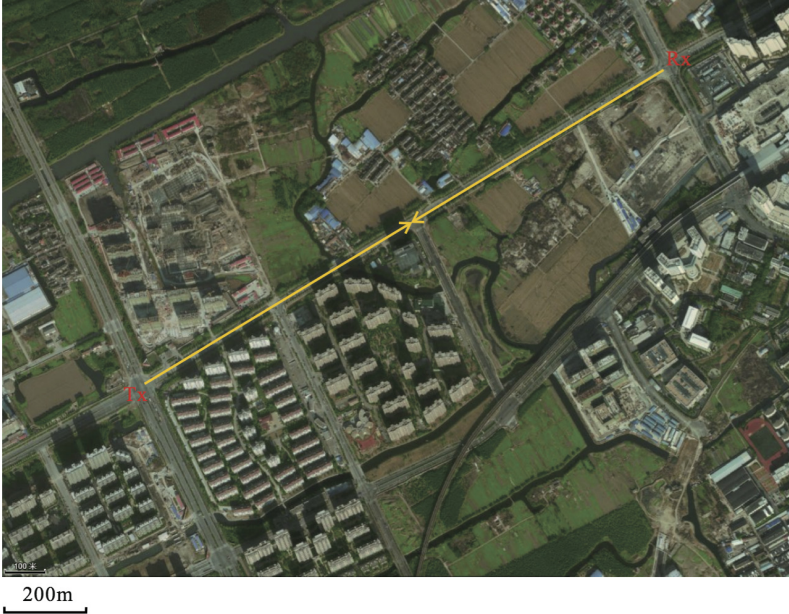

Fig. 3. Satellite map of driving route (Color figure online)

Table 1. Measurement specifications

Center frequency	73 GHz	Sounding signal	PN sequence
Bandwidth	409.6 MHz	Sequence length	4095
Antenna height	1.5 m	Antenna type	Horn antenna
Antenna gain	25 dBi	Average speed	60 km/h
HPBW of antenna	10º	Total distance	1.05 km

3   Measurement Results

3.1   Large-Scale Fading

Figure 4 shows the power gain of the narrowband channel after averaging out the fast fading. The black curve represents the results obtained through the measurements, and
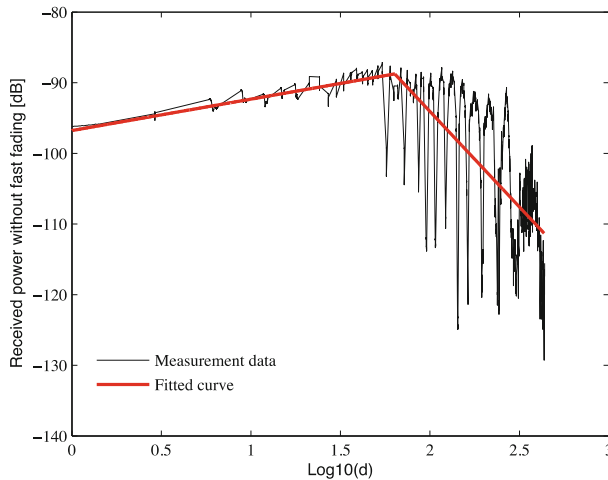
Fig. 4. Narrow-band power after removing fast fading and its fitted curve (Color figure online)

the red curve with analytical expressions is fitted to the black curve in terms of the least-mean-square sense. The expression of the fitted curve is:

$$PL(d) = \begin{cases} 4.4 \cdot \log(d) - 96.8 & 0 < d < 63 \text{ m} \\ -27.0 \cdot \log(d) - 40.0 & 63 \text{ m} < d < 437 \text{ m} \end{cases} \tag{1}$$

Obviously, the fitted curve can be divided into 2 parts. It should be noted that in the first part, the power increases as the distance enlarges. This is of course not the exact characteristics of pure propagation channels, since the HPBW of horn antenna is only 10º which creates a strong directional selectivity. Furthermore, two cars were driven in different lanes, which leads to the occasions that the Rx and Tx are not aligned when two cars are close to each other. In those cases, an obviously lower received power is observed due to the misalignment. In the second part of the fitted curve, it can be observed that the received power declines with significant fluctuations as the Tx-Rx distance increases. This severe variation behavior is mainly caused by the influence of vehicles existing nearby. The obstruction from cars was randomly present. Hence, the shadowing caused by vehicles was also random, which leads to the fluctuation of received power. Figure 5 demonstrates the cumulative distribution function (CDF) of the shadowing existing in the 2 parts respectively. It can be clearly observed that the shadowing in the second part is much larger than the first one. This is reasonable since the shadowing is mainly caused by obstruction, and the obstruction due to cars in the later portion of the curve happens more frequently in our measurement campaign.
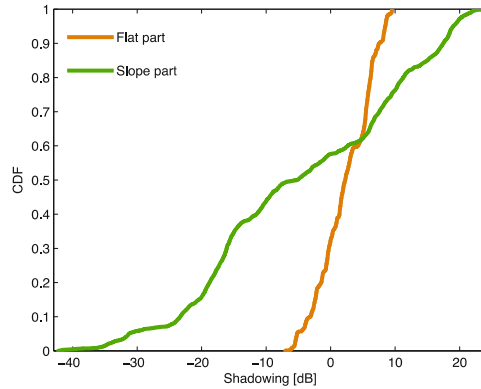
Fig. 5. CDFs of shadowing

3.2 Small-Scale Fading

Small-scale fading is also termed as the fast fading or multi-path fading in literature [25]. In our work, we adopted a distance window with the length of 40 wavelengths to study the statistics of a group of fast fading samples observed through the window. The Kolmogorov-Smirnov (K-S) test is used to find the best fitted distribution for the fast fading coefficients [26]. Six distribution functions of known expressions, i.e., Nakagami, Lognormal, Rician, Rayleigh, Gamma and Weibull are applied. The distribution with minimum K-S statistics is regarded the best-fitted among these options. Figure 6 illustrates the best-fitted distribution for the fast fading at different distances. It can be observed that in the measurements considered here, the best-fitted distribution of fast fading varies when the Tx-Rx distance changes. Figure 7 illustrates the Probability Density Function (PDF) of best fitted distribution. Most groups of fast fading follow lognormal distributions. In addition, most lognormal distributions are found when the
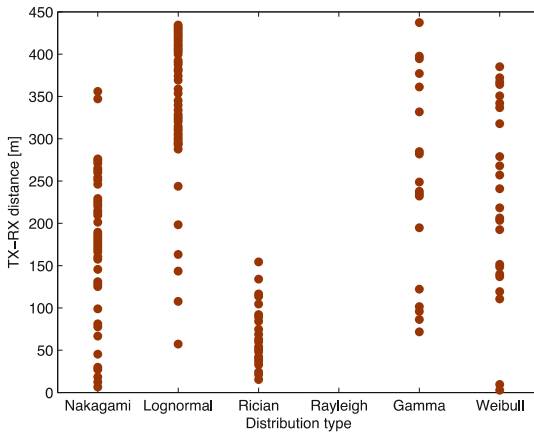
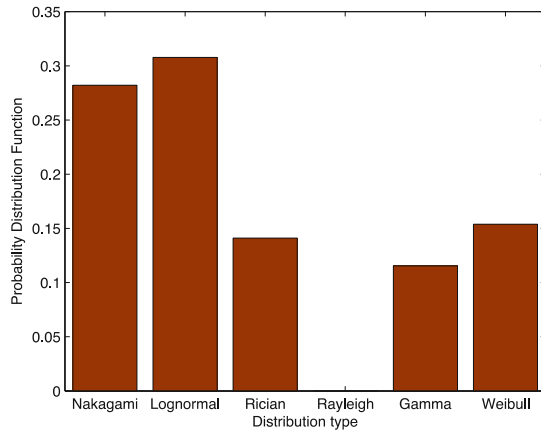

Fig. 6. Distributions of fast fading vs Tx-Rx distance
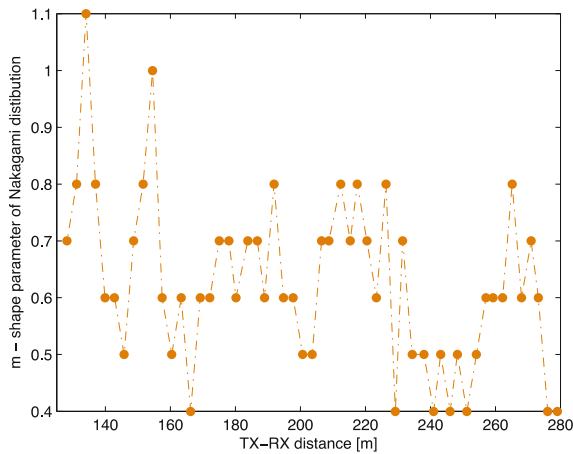
Fig. 7. The PDF of fast fading coefficients

Fig. 8. Nakagami m-factor vs Tx-Rx distance

Tx- Rx distance is larger than 288 m. When the Tx-Rx distance is between 120 m and 288 m, most groups of fast fading follow Nakagami distributions. The m-parameter of Nakagami distribution is reported in Fig. 8. It can be observed from Fig. 8 that the values of m decrease as the Tx-Rx distance increases. This implies that the fast fading becomes severer when two vehicles move away from each other. The fast fading is regarded worse than Rayleigh, since almost all m-parameters are less than 1 [27]. When the distance is less than 120 m, most groups of fast fading follow Rician distribution. Figure 9 demonstrates the Rician K-factor versus the Tx-Rx distance. It is interesting to find that the Rician K-factor increases firstly and then decreases. The breaking point is about 50 m. Two possible reasons are postulated as follows. One is that the car surfaces cause lots of multi-path components when the two cars are close to each other. The
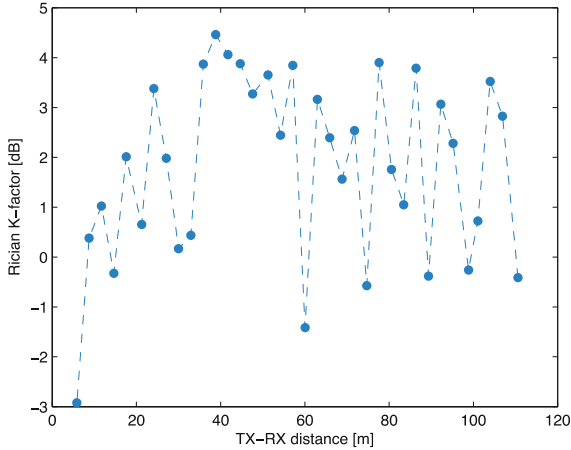
Fig. 9. Rician K-factor vs Tx-Rx distance

other one is because Tx is not aligned with Rx. When the distance is larger than 50 m, more multi-path components caused by other vehicles or scatterers in the scenario can be captured by the antenna with higher probability, which leads to the decrease of the Rician K-factor.

4   Conclusions

A road measurement campaign of V2V channel measurement at 73 GHz was conducted in this work. The study was focused on the channel fading in terms of large-scale fading and small-scale fading phenomena. A 2-slope path-loss model was proposed and the breaking point was found at 63 m. Due to the obstruction of vehicles, the shadowing of the later portion of the model is much larger than in the first part. As for the fast fading, when the distance of two vehicles is less than 120 m, fast fading coefficients follow Rician distributions with higher probability. By computing the Rician K-factors, we can infer that as the distance of two vehicles increases, the LOS component become stronger first and then weaker during this distance range. Here, the breaking point is observed to be about 50 m. When the distance is between 120 and 288 m, the fast fading follows Nakagami distributions. By observing the m-parameter of Nakagami distribution, it can be known that the multi-path fading from cars nearby is insignificant as two cars are close to each other. When the distance is larger than 288 m, most samples of fast fading follow lognormal distributions. These findings can be adopted for generating time-variant channel realizations for evaluating mm-wave V2V communication systems and technologies.

References

1. Giordani, M., Zanella, A., Zorzi, M.: Millimeter wave communication in vehicular networks: challenges and opportunities. In: International Conference on Modern Circuits and Systems Technologies, pp. 1–6 (2017)
2. Viriyasitavat, W., Boban, M., Tsai, H.M., Vasilakos, A.: Vehicular communications: survey and challenges of channel and propagation models. IEEE Veh. Technol. Mag. **10**(2), 55–66 (2015)
3. Cheng, X., Yang, L., Shen, X.: D2D for intelligent transportation systems: a feasibility study. IEEE Trans. Intell. Transp. Syst. **16**(4), 1784–1793 (2015)
4. Fallgren, M., Timus, B.: Scenarios, requirements and KPIs for 5G mobile and wireless system (2013)
5. Yin, X., Cheng, X.: Propagation Channel Characterization, Parameter Estimation, and Modeling for Wireless Communications. Wiley-IEEE Press (2014)
6. Cheng, X., Wang, C.X., Laurenson, D.I., Salous, S., Vasilakos, A.V.: An adaptive geometry-based stochastic model for non-isotropic MIMO mobile to mobile channels. IEEE Trans. Wirel. Commun. **8**(9), 4824–4835 (2009)
7. Patzold, M., Hogstad, B.O., Youssef, N.: Modeling, analysis, and simulation of MIMO mobile to mobile fading channels. IEEE Trans. Wirel. Commun. **7**(2), 510–520 (2008)
8. Liang, X., Zhao, X., Li, S., Wang, Q., Lu, W.: A 3D geometry-based scattering model for vehicle to vehicle wideband MIMO relay-based cooperative channels, vol. 13, no. 10, pp. 1–10 (2016)
9. Cheng, X., Yao, Q., Wen, M., Wang, C.X., Song, L.Y., Jiao, B.L.: Wideband channel modeling and intercarrier interference cancellation for vehicle-to-vehicle communication systems. IEEE J. Sel. Areas Commun. **31**(9), 434–448 (2013)
10. Zhao, X., Liang, X., Li, S., Ai, B.: Two-cylinder and multi-ring GBSSM for realizing and modeling of vehicle-to-vehicle wideband MIMO channels. IEEE Trans. Intell. Transp. Syst. **17**(10), 2787–2799 (2016)
11. Li, Y., He, R., Lin, S., Guan, K., He, D., Wang, Q., Zhong, Z.: Cluster-based non- stationary channel modeling for vehicle-to-vehicle communications. IEEE Antennas Wirel. Propagation Lett. **PP**(99), 1 (2016)
12. Yuan, Y., Wang, C.X., He, Y., Alwakeel, M.M., Aggoune, E.H.M.: 3D wideband non-stationary geometry-based stochastic models for non-isotropic MIMO vehicle to vehicle channels. IEEE Trans. Wirel. Commun. **14**(12), 6883–6895 (2015)
13. Guan, K., Ai, B., Nicolas, M.L., Geise, R., Muller, A., Zhong, Z., Kurner, T.: On the influence of scattering from traffic signs in vehicle-to-x communications. IEEE Trans. Veh. Technol. **65**(8), 5835–5849 (2016)
14. Ghazal, A., Yuan, Y., Wang, C.X., Zhang, Y., Yao, Q., Zhou, H., Duan, W.: A non-stationary IMT-advanced MIMO channel model for high-mobility wireless communication systems (2017)

15. Azpilicueta, L., Aguirre, E., Falcone, F., Lopez-Iturri, P., Alejos, A.V.: Radio channel characterization of vehicle-to-infrastructure communications at 60 GHz. In: International Conference on Electromagnetics in Advanced Applications (2015)
16. He, R., Renaudin, O., Kolmonen, V.M., Haneda, K., Zhong, Z., Ai, B., Oestges, C.: A dynamic wideband directional channel model for vehicle to vehicle communications. IEEE Trans. Industr. Electron. **62**(12), 7870–7882 (2015)
17. Ibdah, Y., Ding, Y.: Mobile-to-mobile channel measurements at 1.85 GHz in suburban environments. IEEE Trans. Commun. **63**(2), 466–475 (2015)
18. Cheng, L., Henty, B.E., Stancil, D.D., Bai, F., Mudalige, P.: Mobile vehicle-to-vehicle narrow-band channel measurement and characterization of the 5.9 GHz dedicated short range communication (DSRC) frequency band. IEEE J. Sel. Areas Commun. **25**(8), 1501–1516 (2007)
19. Walter, M., Fiebig, U.C., Zajic, A.: Experimental verification of the non-stationary statistical model for V2V scatter channels. In: Vehicular Technology Conference, pp. 1–5 (2014)
20. Shemshaki, M., Lasser, G., Ekiz, L., Mecklenbrauker, C.: Empirical path loss model fit from measurements from a vehicle-to-infrastructure network in Munich at 5.9 GHz. In: IEEE International Symposium on Personal, Indoor, and Mobile Radio Communications, pp. 181–185 (2015)
21. He, R., Molisch, A.F., Tufvesson, F., Wang, R., Zhang, T., Li, Z., Zhong, Z., Ai, B.: Measurement-based analysis of relaying performance for Vehicle-to-Vehicle communications with large vehicle obstructions. In: Vehicular Technology Conference, pp. 1–6 (2017)
22. Petrov, V., Kokkoniemi, J., Moltchanov, D., Lehtomaki, J., Juntti, M., Koucheryavy, Y.: The impact of interference from the side lanes on mmwave/THz band V2V communication systems with directional antennas. IEEE Trans. Veh. Technol. **PP**(99), 1 (2018)
23. Blumenstein, J., Prokes, A., Vychodil, J., Pospisil, M., Mikulasek, T.: Time-varying k factor of the mm-wave vehicular channel: velocity, vibrations and the road quality influence. In: 2017 IEEE 28th Annual International Symposium on Personal, Indoor, and Mobile Radio Communications (PIMRC), pp. 1–5, October 2017
24. Park, J.J., Lee, J., Liang, J., Kim, K.W., Lee, K.C., Kim, M.D.: Millimeter wave vehicular blockage characteristics based on 28 GHz measurements. In: 2017 IEEE 86th Vehicular Technology Conference (VTC-Fall), pp. 1–5, September 2017
25. Cai, X., Peng, B., Yin, X., Perez, A.: Hough-transform-based cluster identification and modeling for V2V channels based on measurements. IEEE Trans. Veh. Technol. **PP**(99), 1 (2017)
26. Millard, J., Kurz, L.: The Kolmogorov-Smirnov tests in signal detection (corresp.). IEEE Trans. Inf. Theory **13**(2), 341–342 (1967)
27. Goldsmith, A.: Wireless Communications (2007)